Analytical and experimental study of electrical conductivity in the lithium tantalate nonstoichiometric structure

S. Jebbari[1,2], S. El Hamd[1], F. Bennani[3], A. Jennane[1], M. Hafid[2]and N. Masaif[1]
[1] *L.M.M, Laboratoire de Magnétisme et des Matériaux, Département de Physique Appliquée, Faculté des Sciences et Techniques, B.P. 577 Settat, Morocco*
[2] *LPTN, Département de Physique, Faculté des Sciences Semlalia, B.P. S15 Marrakech, Morocco*
[3] *LPVC, Département de Physique, Faculté des Sciences, B.P. 133 Kénitra, Morocco*

We have been interested to experimental and analytical studies of ionic conductivity of nonstoichiometric $LiTaO_3$ solid solutions. Theoretical approach combined with lithium and tantalate vacancy models has been performed. A comparative study between the calculated and measured values is presented taking into account the temperature and composition effects on the conductivity.

I. Introduction

Lithium tantalate has been the subject of many theoretical and practical investigations due to their properties in electro-optics, electo-acoustics and non-linear optics. This material shows a ferroelectric behaviour well known to deal nonstoichiometric compound. In $LiTaO_3$, the solid solubility range extends from about 46 to 50.4 mol % of Li_2O at room temperature [1].

The structure of ferroelectric's $LiTaO_3$ belongs to space group R3c and can be considered as a superstructure of the α-Al_2O_3 corundum structure with Li^+ and Ta^{5+} cations along the c-axis [2].

Several studies have reported on the changes in electrical conductivity of the lithium tantalate solid solutions [3-6]. By complex impedance spectroscopy; Huanosta et al [4] studied the variation of the conductivity as a function of the stoichiometry in $Li_{1-5x}Ta_{1+x}O_3$ compounds.

In previous work [7], the successive phase transitions corresponding to the various compositions in $LiTaO_3$ system have been re-examined. In brief, ceramic specimens of $LiTaO_3$ with different compositions are studied by the impedance spectroscopy in the 1Hz-1MHz frequency range and the 500-1200 K temperature range. The temperature dependence of the dielectric permittivity of these specimens was measured in order to determine the temperature of the phase transition. So, the ionic conductivity is determined for all compositions from Cole-Cole diagrams. The analysis of the ceramic samples, which are prepared from Li_2O and Ta_2O_5, indicates that there is a modification of the ionic conductivity of $LiTaO_3$ with compositions.

To find which defect is involved in this phenomenon, we have proposed a theoretical description of the defect structure in $LiTaO_3$ on the basis of a set of vacancy models combined with a ferroelectric phase transition theory.

As $LiTaO_3$ is isomorphous with $LiNbO_3$, several defect models have been proposed for $LiNbO_3$.

Fay et al. [8] describe a ceramic sample assumed containing oxygen and lithium vacancies by the oxygen vacancy model having a formula $[Li_{1-2x}\square_{2x}][Nb][O_{3-x}\square_x]$ where [.] represent the sublattice and $\square$ denotes the vacancies. This model cannot describe the density variation in function of the composition. In order to correct this anomaly, Lerner et al. [9] have predicted that an excess of niobium ions might occupy the lithium sites. This is, the lithium vacancy model, which is given by the formula $[Li_{1-5x}Nb_x\square_{4x}][Nb]O_3$ where the lithium vacancies are introduced taking into accounts the charge compensation. However, Peterson and Carnevale [10] observed a new defect structure corresponding to the Nb-site vacancy type using the NMR technique. Then, their niobium vacancy model is arranged as follows: $[Li_{1-5x}Nb_{5x}][Nb_{1-4x}\square_{4x}]O_3$. Contrarily to the result pointed out by Abrahams and Marsh [11], Donnerberg et al. [12] proved that the niobium vacancy model is unfavorable to compare the energetic aspect of the defect structure models. A comparative study between the densities of these models allows Iyi et al. [13] to reject the oxygen vacancy model. From this result, we have only used lithium and tantalate vacancy models to describe the defect structures effects on the conductivity.

A theory of ferroelectric's phase transition in the crystal $LiNbO_3$ has been performed to understand and predict the properties of this crystal [14]. In this system, the solution of the dynamic problem of the crystal planes system exhibits the existence of the "soft mode" at the ferroelectric's transition.

II. Experimental results

The experimental technique and the preparation of the solid solutions have been described elsewhere [7]. By the conventional mixed oxide method, the nonstoichiometric $LiTaO_3$ samples were prepared from Li_2CO_3 and Ta_2O_5. Powders were isostatically pressed at 2500 bars to give pellets of 13 mm in diameter and 1 mm in thickness and were sintered at 1500 K for 4h with a heating rate of 100 K/h.

Ceramics were characterised by X-ray diffraction and the microstructure of these samples were

Li/Ta	Experimental formula	Proposed formula (b)	(c)
1	$LiTaO_3$	$[Li_{1.0}][Ta_{1.0}]O_3$	$[Li_{1.0}Ta_{1.0}]O_3$
0.976	$Li_{0.98}Ta_{1.005}O_3$	$[Li_{0.98}Ta_{0.02}][Ta_{0.985}\blacksquare_{0.015}]O_3$	$[Li_{0.98}Ta_{0.005}\blacksquare_{0.015}][Ta]O_3$
0.95	$Li_{0.958}Ta_{1.008}O_3$	$[Li_{0.958}Ta_{0.042}][Ta_{0.966}\blacksquare_{0.034}]O_3$	$[Li_{0.958}Ta_{0.008}\blacksquare_{0.034}][Ta]O_3$
0.88	$Li_{0.90}Ta_{1.02}O_3$	$[Li_{0.90}Ta_{0.10}][Ta_{0.92}\blacksquare_{0.08}]O_3$	$[Li_{0.90}Ta_{0.02}\blacksquare_{0.08}][Ta]O_3$

Table 1 : Chemical formula obtained by the analysis and the proposed formula according to (b) and (c) models with different Li/Ta ratios.

Among of the electrical measurements investigated, we have interested about the variation of the conductivity σ by complex impedance spectroscopy. The isothermal measurements were carried out between 600 and

1200 K with temperature steps of 50 or 100 K except in T_c range where steps were reduced to 20 K. The range of measuring frequencies was 1Hz-1MHz for ceramic samples. A Pt(Rh 10%)/Pt thermocouple located near the sample is connected to a Keithley 2000 electrometer to measure temperatures; reported temperatures are estimated as accurate to $\pm$ 2K.

The ionic conductivity is determined for all compositions from Cole-Cole diagrams and the variation vs temperature is studied as a function of the Li/Ta ratio [7].

The measured conductivities for nonstoichiometric $LiTaO_3$ with different compositions were shown in FIG.1 the form of Arrhenius plots for the temperature range from 830 to 1250 K.

The curves are essentially linear and permit to determine the activation energy of the studied concentrations. The obtained values are presented in table 2.

examined using scanning electron microscopy (SEM). The chemical composition of the samples was obtained using inductively coupled plasma-atomic emission spectroscopy (ICP-AES).

The formulae obtained, which estimated to be about 0.8% for Li and 0.1% for Ta, are reported in Table 1. We denote by (a), (b) and (c) the oxygen, tantalate and lithium vacancy models.

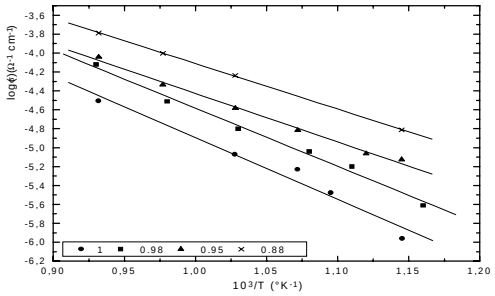

FIG. 1 : Variation of $\log(\sigma)$ as a function of $10^3/T$.The full circles, squares, triangles and crosses are experimental data and the solid lines are the linear fits to the data.

III. Theoretical approach

In this work, we suppose that ceramic samples of $LiTaO_3$ are single crystal. Such an assumption is based on the experimental fact that the ferroelectric's phase transition occurred in the ceramic samples which are formed by parallel planes along the polar "c" axis. In Figure 2, distances between planes (Li, Ta and O at T=0 K) are denoted as follow: $R_{O\text{-}O}$(b= 2.30Å), $R_{Li\text{-}O}$(R_{20}= 0.601 Å), $R_{Ta\text{-}O}$(R_{10}= 0.954 Å), $R_{Li\text{-}Ta}$(R_{12}=b - R_{10} - R_{20}) [15].

The essential of the theory of ferroelectric's transition in $LiTaO_3$ is reported in reference [14]. Here we only report the useful expressions in the appendix.

At 0°K, the soft mode frequency, ω^2, is proportional to the Curie temperature. Substituting ω^2 by expression A.10 to obtain the following relation that allows calculating the Curie temperature:

$$\frac{T^*}{T} = \frac{M_1^* + M_2^* + M_0^*}{M_1 + M_2 + M_0}\left(\frac{M_1 M_2 M_0}{M_1^* M_2^* M_0^*}\right)\left(\frac{P_1^*}{P_1}\right)\left(\frac{P_2}{P_2^*}\right) \quad (1)$$

with

$$P_1^* = 3q_0^* R_{12}^2 - q_1^* R_{20}^2 - q_2^* R_{10}^2$$

and

$$P_2^* = \frac{(R_{20}R_{21})^2}{q_2^*}\left(\frac{1}{M_1} + \frac{1}{M_0}\right) + \frac{(R_{10}R_{21})^2}{q_1^*} \times \left(\frac{1}{M_2} + \frac{1}{M_0}\right) - \frac{(R_{10}R_{20})^2}{3q_0^*}\left(\frac{1}{M_1} + \frac{1}{M_2}\right)$$

The elements X and X^* related to exactly stoichiometric and nonstoichiometric compositions respectively.

This expression allows to determinate Curie temperatures of the defect structure models.

Electrical conductivity can be described by the law Arrhenius,

$$\sigma = \sigma_o \exp\left(-\frac{\Delta E}{k_B T}\right) \quad (2)$$

where σ_0 is the pre-exponential factor, ΔE the activation energy, k_B the Boltzmann constant and T is the temperature (K).

We introduce the conductivity, σ^*, to explain the role of defect structure in nonstoichiometric lithium tantalate compound.

Li/Ta	Activation energy (eV)	$\log(\sigma_o)$ ($\Omega^{-1}cm^{-1}$)
1	1.16	0.88
0.98	1.14	1.18
0.95	0.91	0.11
0.88	0.86	0.19

Table 2 : Values of the activation energy and $\log(\sigma_o)$ of the $LiTaO_3$ for the different Li/Ta ratios studied.

$$\sigma^* = \sigma_o^* \exp\left(-\frac{\Delta E^*}{k_B T^*}\right) \quad (3)$$

Although the expression of the T^* is determinate at Curie temperature point, this relation seems again

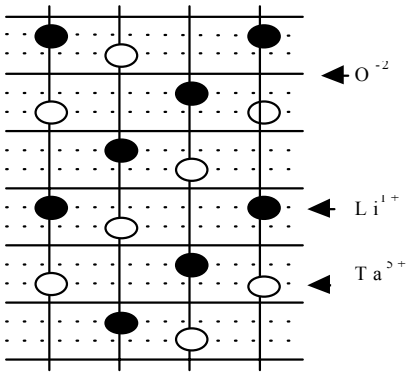

FIG. 2 : Different planes in an elementary cell of crystal $LiTaO_3$.

correct to calculate the conductivity about T^*.

Taking into account of the experimental results, we have proposed two possible models: tantalate and lithium vacancy models.

However, we represent these models, described previously, in the following condensed form, $[Li_{\alpha_1}Ta_{\alpha_2}\square_{\alpha_3}][Ta_{\beta_1}\square_{\beta_2}][O_{3\gamma_1}\square_{\gamma_2}]$; and $K^* = g\,K$ with K=M, q and g= α, β or γ. Here α, β and γ allow identifying two models as follows:

i) Tantalum vacancy model corresponds to α_1=1-5x, α_2=5x, β_1=1-4x, β_2=4x and γ_1=1; and $K_2^* = (1-5x)K_2 + 5xK_1$, $K_1^* = (1-4x)K_1$ and $K_0^* = K_0$.

ii) Lithium vacancy model corresponds to α_1=1-5x, α_2=x, α_3=4x, β_1=1 and γ_1=1; and $K_2^* = (1-5x)K_2 + xK_1$, $K_1^* = K_1$ and $K_0^* = K_0$.

In this representation α=β=γ=0 signified that ions and vacancies are absent in these nonstoichiometric models.

In order to provide an adequate description of defect structure in nonstoichiometric lithium tantalate we have analytically performed the calculations of the Curie temperature as function of the composition x that we illustrate in Table 3. Estimate values of T^* for $LiTaO_3$ have been obtained using the following values of charges and masses of ions $q_0=2$, $q_1=5$, $q_2=1$, $M_0=48$, $M_1=180.95$, $M_2=6.94$.

The conductivities for these vacancy models could, therefore, be calculated according to equation (3) taking into account the values of the σ_0 and ΔE for each composition x.

	(b)	(c)
T_c^*	$\frac{(1-17.88\,x)(1+0.62\,x)(1+20\,x)}{(1+78.01\,x)}\,T_c$	$\frac{1+0.62\,x}{1+18.26\,x}\,T_c$

Table 3 : The Curie temperature T^* as a functic
(b) and (c) represent th

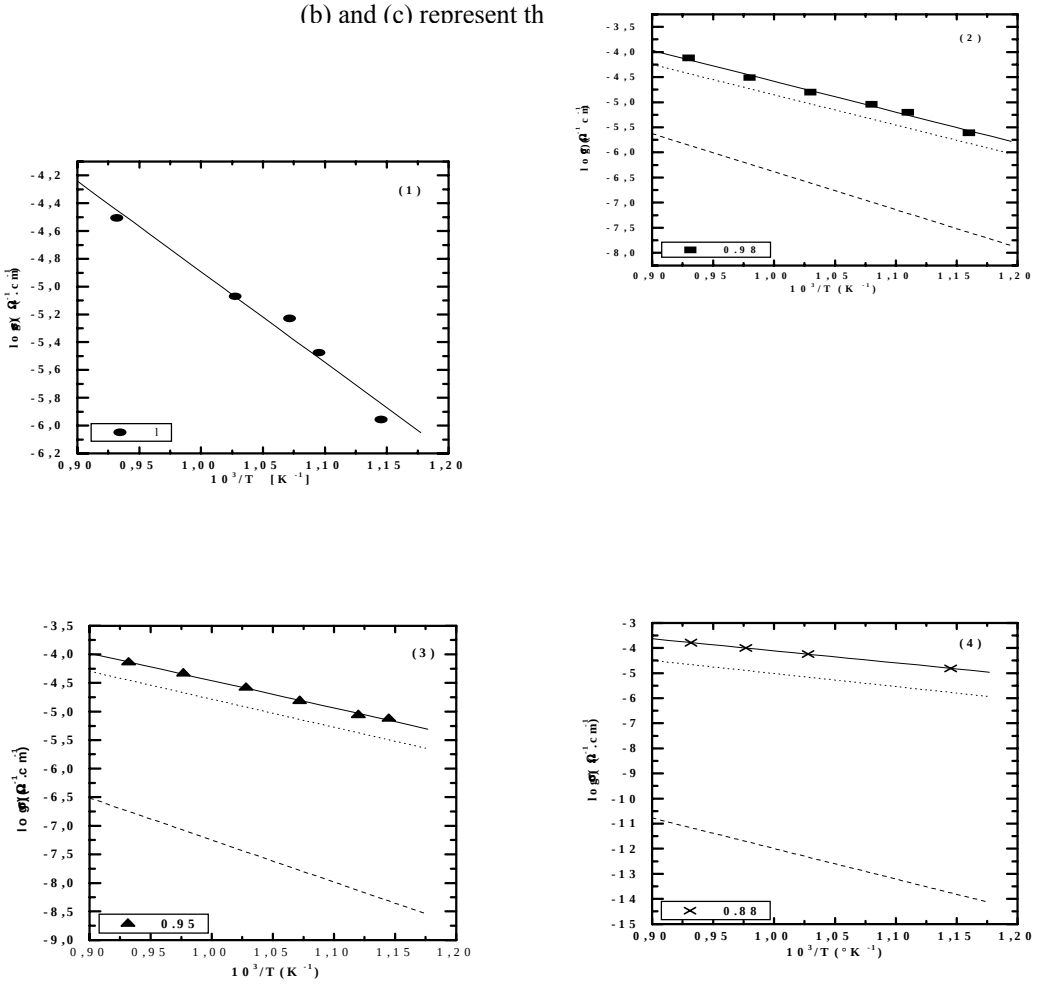

FIG. 3 : Logarithmical conductivity of $LiTaO_3$ solid solutions as function of the reciprocal temperature with different composition x. (1) Li/Ta=1, (2) Li/Ta=0.98, (3) Li/Ta=0.95 and (4) Li/Ta=0.88. The full circles, squares, triangles and crosses are experimental data and the solid lines represent the linear fits to the data. Dash and dot lines indicate the linear fits of (b) and (c) models respectively.

IV. Results and discussion

By a linear fit of the experimental values and the calculation of the slope of the curve logσ in the form of Arrhenius plot (figure 1) we obtained σ_0 and ΔE for each composition x. Estimated activation energy at different Li/Ta ratio from equation (2) is reported in Table 2.

Calculated and experimental values of σ* for various nonstoichiometric compositions are illustrated in Figures 3. A comparison of the measured conductivity with two vacancy models (Lithium and tantalate vacancy models) is indicating.

Observed curves log(σ) vs T^{-1} indicate that the lithium vacancy model is the best to describe the conductivity in nonstoichiometric $LiTaO_3$ solid solutions. Effect of the lithium defect is predominant over that of tantalate vacancies in the conductivity of the $LiTaO_3$. Thus, the number of Li vacancies connected with the composition Li/Ta ratio is mainly responsible for the increase found in conductivity.

V. Conclusion

We have presented conductivity as a function of temperature and composition in nonstoichiometric $LiTaO_3$ ceramics. In this simple system, the theory of ferroelectric's phase transition gives a good quantitative description of the experimental results. A comparative study, between vacancy models and experimental values of the conductivities, shows that the lithium vacancy model is the defect model, which can be suggested to describe the defect structure in nonstoichiometric lithium tantalate.

Appendix

The energy of electrostatic interaction of two charged long lines is,

$$W = e^2 \delta_i \delta_j b^2 \ln \frac{2l}{R_{ij}} \qquad (A1)$$

where $\delta_i = \frac{N_i q_i}{l\, b}$ with l, R_{ij}, q_i and N_i is the line length, the distance between lines, the charge of ions and their number respectively.

We deduce the full energy of interaction of planes such that:

$$U_{ij} = -\frac{e^2 q_i q_j}{b} \ln \frac{2l}{R_{ij}} + \frac{B_{ij}}{R_{ij}^n} \qquad (A2)$$

where $B_{ij} = \frac{e^2 q_i q_j}{b\, n} (R_{ij}^0)^n$ with R_{ij}^0 is the equilibrium distance between planes.

If we put $x_{ij} = R_{ij} - R_{ij}^0$, then the energy writes

$$U_{ij} = \frac{e^2 q_i q_j}{b} \left(\frac{1}{n} - \ln \frac{2l}{R_{ij}^0}\right) + \frac{e^2 q_i q_j n}{b\,(R_{ij}^0)^2} \frac{x_{ij}^2}{2} \qquad (A3)$$

The coefficient $C_{ij} = \frac{e^2 q_i q_j}{b\,(R_{ij}^0)^2} n$ describes the interaction between Li and O planes (as well as for Ta and O).

However, the interaction between Li and Ta will deduce from the total energy:

$$U_{ij} = \frac{e^2 q_i q_j}{b} \ln \frac{2l}{R_{ij}^0} - \frac{B_{ij}}{R_{ij}} \qquad (A4)$$

Finally, for $LiTaO_3$ crystal C_{ij} coefficients are

$$C_{\text{Li-O}} \equiv C_{20} = -3 \frac{q_0 q_2 e^2}{b\, R_{20}^2} n ,$$

$$C_{\text{Ta-O}} \equiv C_{10} = -3 \frac{q_0 q_1 e^2}{b\, R_{10}^2} n ,$$

$$\text{and } C_{\text{Li-Ta}} \equiv C_{21} = \frac{q_1 q_2 e^2}{b\, R_{21}^2} n \qquad (A5)$$

where q_1, q_2 and q_0 are the electric charge of Nb^{5+}, Li^{1+}, and O^{2-} ions, respectively.

To solve the dynamic problem we reduced the structure of charged planes to system of vibration of linear lattice (FIG. 4).

The displacements of the three ions are indicated by v_s (Li^{1+}), u_s (Nb^{5+}) and ξ_s (O^{2-}). Then, the system is described by the differential equations as

$$\begin{aligned} M_1 \ddot{u}_s &= C_{10}(\xi_{s+1} - u_s) + C_{21}(v_s - u_s) \\ M_2 \ddot{v}_s &= C_{21}(u_s - v_s) + C_{20}(\xi_s - u_s) \\ M_0 \ddot{\xi}_s &= C_{20}(v_s - \xi_s) + C_{10}(v_{s-1} - \xi_s) \end{aligned} \qquad (A6)$$

where M_1, M_2, M_0 are the masses of elements Ta, Li and 3O respectively.

The choose of solutions in the form of plan waves,

$$g_s = g\, e^{i(\omega t + a\, s\, k)} \qquad (A7)$$

with g = u, v or ξ

leads to a system of linear equations.

This system has a nontrivial solution. Then we put k=0 in the determinant equation (Δ=0) in order to obtain the fundamental frequencies of optical branches. Then we obtain the following equation,

$\omega^4 - B\,\omega^2 + D = 0$, where:

$$B = C_{10}\left(\frac{1}{M_1}+\frac{1}{M_0}\right) + C_{21}\left(\frac{1}{M_1}+\frac{1}{M_2}\right) + C_{20}\left(\frac{1}{M_2}+\frac{1}{M_0}\right)$$

and $$D = \frac{M_1+M_2+M_0}{M_1M_2M_0} \times (C_{10}C_{20}+C_{10}C_{21}+C_{21}C_{20}) \quad \text{(A8)}$$

The two optical modes are given by

$$\omega_{12}^2 = \frac{1}{2}B \pm \left(\frac{1}{4}B^2 - D\right)^{1/2} \quad \text{(A9)}$$

For small parameter ($(4D/B^2)<<1$) we deduce,

$$\omega_2^2 = \frac{D}{B} = \frac{ne^2}{b}\frac{M_1+M_2+M_0}{M_1M_2M_0}\frac{P_1}{P_2},$$

$$\omega_1^2 = B - \omega_2^2$$

with $P_1 = 3q_0R_{12}^2 - q_1R_{20}^2 - q_2R_{10}^2$

and $$P_2 = \frac{(R_{20}R_{21})^2}{q_2}\left(\frac{1}{M_1}+\frac{1}{M_0}\right) + \frac{(R_{10}R_{21})^2}{q_1} \times \left(\frac{1}{M_2}+\frac{1}{M_0}\right) - \frac{(R_{10}R_{20})^2}{3q_0}\left(\frac{1}{M_1}+\frac{1}{M_2}\right) \quad \text{(A10)}$$

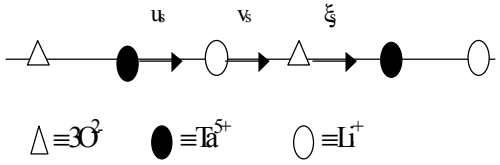

FIG. 4: Displacement of Li^+, Ta^{5+} and $3O^{2-}$ ions in a linear lattice.

References

[1] M. Paul, M. Tabuchi, A. R. West, Chem. Mater., 9 (1997) 3206.
[2] S. C. Abrahams, L. J. Bernstein, Phys. Chem. Solids, 28 (1967) 1685.
[3] Y. Fujino, H. Tsuya, K. Sugibachi, Ferroelectrics, 2 (1971) 113.
[4] A. Huanosta, A. R. West, J. App. Phys., 61 (1987) 5386.
[5] D. C. Sinclair, A. R. West, Phys. Rev. B, 39 (1989) 13486.
[6] I. Tomeno, S. Matsumura, Phys. Rev. B, 38 (1988) 606.
[7] F. Bennani, E. Husson, J of European Cearamic Society, 21 (2001) 847.
[8] H. Fay, W. J. Alford, H. M. Dess, Appl. Phys. Lett., 12 (1968) 89.
[9]P. Lerner, C. Legras, J. P. Dumas, J. Cryst. Growth, 3/4, (1968) 231.
[10] G. E. Peterson, A. Carnevale, J. Chem. Phys., 56 (1972) 4848.
[11] C. S. Abrahams, P. Marsh, Acta Crystallogr. Sect. B, 42 (1986) 61.
[12] H. Donnerberg, S. M. Tomlinson, C. R. A. Catlow, O. F. Schirmer., Phys. Rev. B, 40 (1989) 909.
[13] N. Iyi, K. Kitamura, F. Izumi, J. K. Yamamoto, T. Hayashi, H. Asano, S. Kimura., J. of Solid State chem., 101 (1992) 340.
[14] F. P. Safaryan, Physics Let. A, 191 (1999) 255.
[15] M. E. Lines, A. M. Glass, Principles and application of ferroelectrics and related materials. Clarendon Press, Oxford (1977).